in: Proc. IEEE Int. Conf. on Robotics and Automation (ICRA 2009), Kobe, Japan, pp. 424-429, Omnipress 2009

Autonomous Robot Cameraman - Observation Pose Optimization for a Mobile Service Robot in Indoor Living Space

Christof Schroeter, Matthias Hoechemer, Steffen Mueller, Horst-Michael Gross

***Abstract*— This paper presents a model based system for a mobile robot to find an optimal pose for the observation of a person in indoor living environments. We define the observation pose as a combination of the camera position and view direction as well as further parameters like the aperture angle. The optimal placement of a camera is not trivial because of the high dynamic range of the scenes near windows or other bright light sources, which often results in poor image quality due to glare or hard shadows. The proposed method tries to minimize these negative effects by determining an optimal camera pose based on two major models: A spatial free space model and a representation of the lighting. In particular, a task-dependent optimization takes into account the intended purpose of the camera images, e.g. different inputs are needed for video communication with other people or for an image-processing based passive observation of the person's activities. To prove the validity of our approach, we present first experimental results comparing the chosen observation pose and resulting image with and without respect to lighting in different observation tasks.**

I. Introduction

The work presented here is developed in the context of a mobile robot assisting elderly and solitary people in their living space, which serves as an interaction partner and provides services like reminders for medicaments or cognitive and physical stimulation programs. Another important function is the possibility for the user to stay in contact with relatives, friends and doctors or care givers through the use of video phone technology. For many of these purposes, the robot has to observe the person by means of a camera, either to extract information from the input image or to relay the video data to a communication partner. In this paper, we will consider only two exemplary observation tasks specified as follows:

Video Conference: The person is using the robot as a mobile video phone terminal. For that purpose, the robot must stand close to the user, in order to allow him a good view of the attached display. Furthermore, the image aquired by the robot should provide a high contrast view on the person's face and the upper part of the body. The image quality must be targetted at the human observer.

Passive Observation: This is an important task for the mobile robot, e.g. to estimate the state of the observed person and detect alarm conditions. In this operation mode, the robot should choose a non-disturbing location in the background. The observable area should be large to avoid the need for position changes when the person moves around. The necessary image quality depends on the employed machine vision algorithms.

Notice, however, that the proposed approach is not limited to these two tasks, any number of tasks with different requirements can be defined and integrated.

Most existing methods for an autonomous task driven camera positioning system (active camera control) take into account only the pose of the target and focus on detecting the position of persons. For mobile robot applications, some approaches additionally consider obstacles in the environment [1], [2]. However, most of them assume that the resulting image quality depends on the image composition only.

In contrast to that, we claim that the quality of natural images is mainly determined by the illumination and its distribution. A minimum amount of illumination is needed in order to take a picture of a scene, while too bright light can result in glare effects. The central issue in human living space is the high dynamic range of the scenes, particularly for digital camera systems. Unlike the human eye, digital cameras have strong limitations in reproducing scenes with high contrast. One possible solution is the use of high dynamic range (HDR) cameras. Other proposed solutions, like the automatic sensor placement presented in [3] and [4], depend on a high–precision CAD model of the environment and extensive control over scene lighting, which is not available in mobile robot applications. Another aspect that has not been considered before is the convenience of the cameraman pose for the user, e.g. if the person is glared by direct sunlight during interaction with the robot, the pose is suboptimal even with good camera image quality.

In this paper, we will take some aspects for granted, which we have expertise in, but will not further discuss here:

- a metric representation (map) of the environment [5]
- self-localization of the robot within the environment [6]
- navigation skills of the robot like path planning and obstacle avoidance [7]
- pose estimation [8] and segmentation [9] of persons

II. Overview

The aim of this work is to optimize the pose for an autonomous cameraman. The variable to optimize is called observation pose, which theoretically consists of the position of the camera (x, y, z), yaw φ, pitch θ and aperture angle γ. However, due to memory complexity and update cost, in this work we only consider a two–dimensional environment

M. Hoechemer, C. Schroeter, S. Mueller, and H.-M. Gross are with Institute of Neuroinformatics and Cognitive Robotics, Technical University of Ilmenau, Germany. The research leading to these results has received partial funding from the European Community's Seventh Framework Programme (FP7/2007-2013) under grant agreement no. 216487 (CompanionAble-Project).

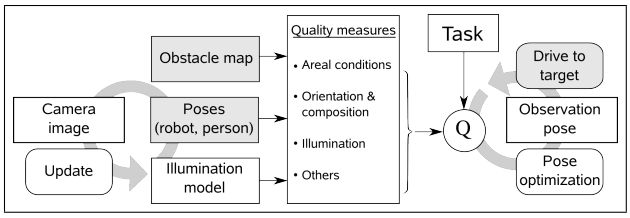

Fig. 1. Overview of the proposed system: The robot continuously updates the illumination model (while driving) using camera images. After receiving an observation task, the robot optimizes the quality function Q to obtain a possible video pose and drives to the target.

model, which results in a restricted observation pose as well:

$$\mathbf{P}_{vid} = (x, y, \varphi, \gamma) \tag{1}$$

Therefore, we only require a fixed mounted camera at a mobile robot with control of the aperture (focal length). With a more complex modelling of the lighting, it is also possible to include actions which allow illumination control, e.g. switching light sources or window blinds.

The problem of finding an optimal observation pose for a task can be formulated as a general optimization problem. The aim is to find a camera pose providing an optimal image quality, while taking into acount the constraints given by the observation task and the environment. In general, there are three optimization approaches: model free, model based and hybrid systems. For a predictive approach, a model of the environment is needed. In the absence of any model, the robot would either have to randomly select camera poses and evaluate the quality of the images, until a sufficient pose is found, or it could apply local optimization methods like gradient descent [10]. Both approaches could result in a lengthy search process, and would not guarantee global optimality. In contrast, the environment model should allow the robot to predict the expected image quality at any position and find an optimal pose for a given task before starting to move. To that purpose, the lighting model is generated and constantly updated from observations (section III).

In order to allow the evaluation of the overall quality of a certain pose, we define metrics for the respective influence factors (subsection IV-A). A task-dependent optimality criterion is defined, and, given the metrics, an optimization process is employed to find the best observation pose (subsections IV-B, IV-C). Fig. 1 shows a system overview.

III. Illumination Model

The illumination model will be used to predict the image quality at a given location within the operational area. For this purpose, the luminance (brightness) distribution of relevant object surfaces is modelled. As we are assuming a camera with fixed height and no pan angle, a two-dimensional illumination model is sufficient, similar to a 2D obstacle grid map. For the basics of photometry, we refer the reader to [11]. The luminance of an object surface at position (x, y) depends on the observer direction φ:

$$L = f(x, y, \varphi) \tag{2}$$

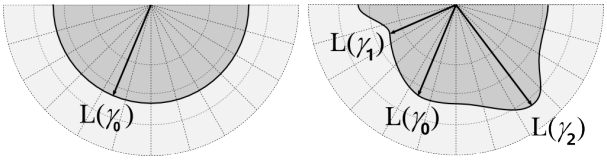

Fig. 2. Model representation of luminance distribution (virtual light source) at a certain position (x, y). Lambertian after one observation (left), multimodal distribution after three observations (right).

The surfaces for which the luminance distribution is represented must be pre-defined, e.g. by manual labeling or automatic extraction from the environment map, usually these are the walls and large static obstacles. The lighting upon these surfaces is represented by virtual discrete light sources (Fig. 2 and 6). Each virtual light source l is defined by its position (x_l, y_l) and a luminance distribution $L_l(\varphi)$. While for most secondary light sources (reflectors), like walls, the assumption of a lambertian characteristic $L_l(\varphi) = c$ is justified, this is not sufficient for primary light sources, like lamps and also windows. Obviously, for a lambertian object the luminance distribution $L_l(\varphi)$ is known from a single observation at any view angle φ. In order to allow estimation of a precise distribution from a small number of observations for objects with unknown luminance characteristics, we introduce the so-called generalized lambertian model (Fig. 2).

A. Generalised Lambertian Model

The generalised lambertian model allows an approximation of the luminance distribution $L(\varphi)$ from a small number of observations from different directions φ (Fig.2). The model is based on the following principles:

- assume lambertian characteristic if only one observation is available
- estimate a multi-modal distribution from multiple observations
- influence of observations decreases with time elapsing

The first principle is a good approximation for the unknown emission characteristics of surfaces observed only from one direction. If observations from more directions are available, the model has to adapt, in order to estimate a more realistic luminance distribution. The third assumption is based on the fact that the luminance distribution of light sources may change over time (e.g. windows due to sun movement), therefore older observations have lower probability of reflecting the current luminance correctly.

These requirements are met by a reference observation based model of the lighting: The continous direction space in the range of $\pm\pi/2$ (relative to the surface normal) is divided into N discrete sectors. Each sector i stores for its respective direction the most recent observed luminance L_i^o and the observation time t_i^o. The estimated luminance L_i^{est} for an arbitrary direction (sector i) can now be inferred at time t from the stored observations as follows:

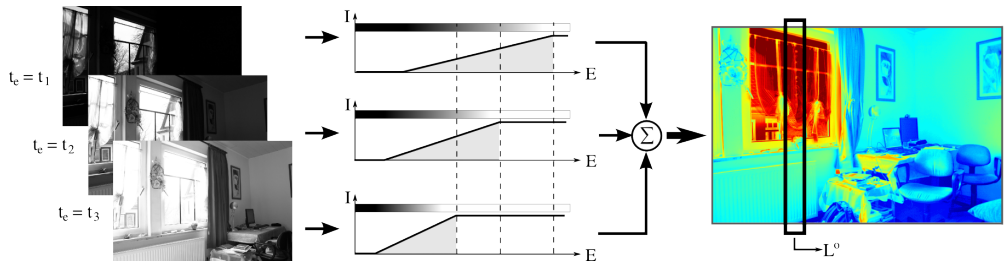

Fig. 3. Calculation of a luminance image from a sequence of exposures $t_1 < t_2 < t3$: Each image covers a particular lumination range. An HDR image (right, false color rendering) is computed using only non–saturated pixels from each image. The number of images in the sequence should be determined adaptively by histogram evaluation. The average luminance value L^o over a column of the HDR image is used to update the 2D illumination model.

$$L^{est}(t,i) = \frac{\sum_j L_j^o \cdot d(i,j) \cdot w(t,t_j^o)}{\sum d(i,j) \cdot w(t,t_j^o)} \tag{3}$$

$$d(i,j) = \exp\left(-(i-j)^2 \cdot \sigma^{-2}\right) \tag{4}$$

$$w(t,t^o) = \exp\left(-(t-t^o)^2 \cdot \tau^{-2}\right) \tag{5}$$

The estimated luminance L_i^{est} is a weighted mean of all observed values, with distance weights $d(i,j)$ for two sectors i,j and time weights $w(t,t^o)$ for current time t and observation time t^o. Initialization is done by setting all observation times $t_j^o \rightarrow -\infty$.

B. Illumination Model Update from Observations

In the model description we assumed that we are able to observe the luminance of an object. Actually, the computation of luminance values from camera images is not trivial. The *illuminance* E on the camera's sensor is described by

$$E_{cam}(\gamma) = \frac{\pi \cdot \tau_{opt} \cdot L}{1+4K^2} \cdot cos^4(\gamma) \cdot \Omega_0 \tag{6}$$

where τ_{opt} is the optical transmission, L is the luminance of an object, K is the aperture (f–number) and γ is the light's arriving angle. Ω_0 is the unit solid angle and is just used as a unit normalizer. Note that vignetting effects have to be corrected for consistent luminance measurements over the entire image and that the resulting intensity value I is not dependent on the illuminance but on the *exposure* H. For short exposure time t_e, H is a linear function of E. Finally, the pixel intensity value I produced by the camera is a function of exposure H, which can be determined by calibration:

$$I = f(H) = f(E_{cam} \cdot t_e) \tag{7}$$

With known relation f between exposure and gray value, the observed luminance L^o can be computed combining eq. (6) and (7):

$$L^o = \frac{f^{-1}(I)}{t_e} \cdot \frac{1+4K^2}{\pi \cdot \tau_{opt} \cdot cos^4(\gamma) \cdot \Omega_0} \tag{8}$$

The function f can only be inverted for non-saturated (black or white) intensities, however, because of the high dynamic range of indoor scenes with daylight, camera images tend to have many saturated pixels. One solution would be a High–Dynamic–Range (HDR) camera with local exposure control. Unfortunately, these are more expensive and have other limitations like lower resolution, which results in the need to have multiple dedicated cameras for different purposes. Instead, our approach is to employ HDR techniques with a standard CCD camera [12], [13]. The basic idea is to compute the luminance of a scene not from one single image but from a sequence of exposure times t_e (Fig. 3), in order to exceed the physical dynamic range of the camera.

With the resulting HDR luminance image, a particular virtual light source can be updated calculating L_i^o as the average luminance over the respective image column. The update is done for all visible virtual lights in the model.

IV. Observation Pose Planning

A. Factors of influence

For a quality estimation of observation poses, a number of aspects must be considered. In this subsection, the different classes of influence factors q_i for the suitability of a given observation pose are discussed.

1) Areal conditions: An important factor for mobile robots are all kinds of areal conditions. The robot has to consider obstacles and unreachable positions due to path obstructions. In order to visually observe the person, it is also important to check for visual occlusions. This can be done based on the object surface information which is also used in the illumination model. Note that not all obstacles in the scene need to result in visual occlusions, but most obstacles higher than the camera do so. All these areal conditions will be considered as constraints in the optimization process (subsection IV-C).

2) Orientation & Composition: Another important aspect for a cameraman is the image composition. Here, the person's location in the image and their size related to the image size have to be considered (Fig. 4). The robot view direction with respect to the person's location is called Robot–Person–Angle α. For $\alpha = 0$ the robot looks straight at the observable person, resulting in a centered alignment. As the composition is directly affected by α, we can use it as a factor of influence for the image quality (eq. (9)).

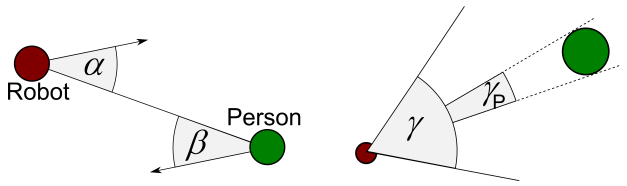

Fig. 4. Relative robot and person orientations (left) and definition of the relative person size (right) by aperture angle γ and person view angle γ_p.

The so called Person–Robot–Angle β is also an influence factor on the quality of the observation pose (Fig. 4 left). For $\beta = 0$ the observation pose is directly in front of the person. $\beta \neq 0$ means the person has to turn his/her head to interact with the robot, which is inconvenient and there is a hard limit of possible head turn. The quality of the observation pose is directly affected by β (eq. (9)).

Furthermore, the relative person (face) size with respect to the size of the image is very important for the image composition (Fig. 4, right). It can be computed as the ratio of the camera view angle γ and the person view angle γ_p.

Based on these observations, quality measures are defined:

$$q_{RPA} = \alpha \qquad q_{PRA} = \beta \qquad q_{size} = \gamma_p/\gamma \tag{9}$$

3) Illumination: A further important group of factors are illumination metrics. The image quality strongly depends on the available illumination. First of all, a minimum amount of light is needed to record naturally looking images, however, too bright light or too strong contrast affect image quality negatively. Here, we mainly focus on avoiding glare and bad visiblity caused by directional light (Fig. 5).

Because of the high dynamic range of indoor living scenes, the major glare component is relative glare. To avoid this effect, we have to limit the difference of the face luminance and the luminance of the image background. The prediction of the background luminance L_{back} is computed directly from the illumination model by determining all virtual lights visible from the hypothetical observer's position. L_{back} can then be computed simply as the average luminance value, or a weighted sum taking into account the dependency of glare on view direction (glare at the image border is far less influencing quality than in the image center). In contrast to that, the face luminance L_{obj} is not represented in the model, but the effect of indirect illumination from the virtual lights can be computed, using the photometric distance law:

$$E_{obj} = \sum_i \frac{L_i\left(\gamma_{1,i}\right) \cdot A \cdot \cos\gamma_{1,i}}{r_i^2} \cdot \cos\gamma_{2,i} \cdot \Omega_0 \tag{10}$$

Fig. 5. Degradation of image quality due to strong glare (left, center) and directional light (right).

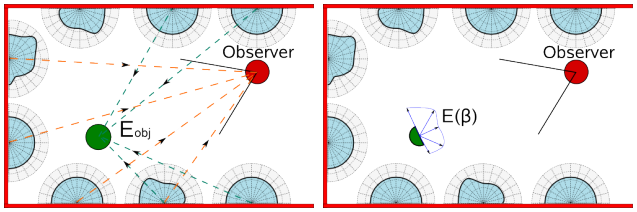

Fig. 6. 2D Illumination model with discrete light sources upon the walls. Left: Calculation for glare metric q_{glare}. Light results in total illumination E on the person's face. The contrast can be computed against the background luminance. Right: Illumination distribution $E(\beta)$ for visibility measure q_{vis}.

Here, $L_i\left(\gamma_{1,i}\right)$ is the luminance of a virtual light source i, A is its surface area, $\gamma_{1,i}$ is the angle between virtual light surface normal and person, $\gamma_{2,i}$ is the angle between persons orientation and light source, and r_i is the distance between light source and person.

With known object reflectivity ρ_{obj} and the assumption that the object's reflectivity is lambertian (approximately true for human faces), the object luminance L_{obj} follows:

$$L_{obj} = \frac{\rho_{obj} \cdot E_{obj}}{\pi \cdot \Omega_0} \tag{11}$$

The glare metric can now be defined as the dynamic range:

$$q_{glare} = \log\left(1 + \frac{L_{back}}{L_{obj}}\right) \tag{12}$$

For an optimal observation pose, we need to take into account glare of the robot and glare of the observed person, because for long interactive tasks, like a video conference, a convenient position should be ensured.

Besides glare, the visibility of the person's face determines the image quality. An unbalanced illumination results in hard shadows (Fig. 5, right). The description of this aspect is similar to the calculation of face illuminance E_{obj} in eq. (10), but in this case the full distribution of the illumination $E(\beta)$ is regarded for the range $-\pi < \beta < \pi$:

$$E(\beta) = \sum_i \frac{L_i\left(\gamma_{1,i}\right) \cdot A \cdot \cos\gamma_{1,i}}{r_i^2} \cdot \cos\left(\gamma_{2,i} + \beta\right) \cdot \Omega_0 \tag{13}$$

The resulting distribution is compared against a desired distribution $\hat{E}(\beta)$ taking into account the desired symmetry and the preference for lateral over frontal lighting (Fig. 7):

$$q_{vis} = \int_{-\pi/2}^{\pi/2} \left(\frac{\hat{E}(\beta)}{\int \hat{E}(\beta) d\beta} - \frac{E(\beta)}{\int E(\beta) d\beta} \right)^2 d\beta \tag{14}$$

4) Others: Other quality measures which cannot be classified in the previously described groups are the Task Valid Area q_{TVA} describing a valid area for task execution, the Wall Distance q_{wall} which is a measure describing the closeness to the walls (for an unobtrusive placement, e.g. in passive observation) and the Inhibited Areas q_{inh}, wich define regions not to use for observation pose (e.g. doors).

B. Optimality criterion

Each of the influence factors describes one aspect of the observation pose quality. To obtain a total quality metric (cost function), these are integrated in a weighted sum:

$$Q^{Task}\left(\mathbf{P}_{vid}\right) = \sum_i w_i^{Task} \cdot f_i^{Task}\left(q_i\right) \tag{15}$$

$$\text{with } q_i = \{q_{obstacles}; q_{PRA}; q_{RPA}; q_{size}; q_{TVA}; q_{glare,R}; q_{glare,P}; q_{vis}; q_{path}; q_{wall}; q_{inh}\}$$

Note that this is not just a linear combination of the influence factors, but the single metrics q_i will be transformed by a commonly non–linear and task dependent transfer function f_i^{Task}. The purpose of this transfer function is to scale the influence factors, define their setpoints and model the nonlinearity of influence factors to observation quality. As an example, task dependence is illustrated for the relative person size q_{size} in Fig. 8.

C. Optimization

Using eq. (15), the quality criterion can be evaluated for any given observation pose. With the definition of task dependent weights and transfer functions, the quality measure can be adapted to reflect the specific requirements of any observation task. Finally, the optimization must be solved:

$$\mathbf{P}_{vid}^{opt} = \arg\min_{\mathbf{P}_{vid}} \left(Q^{Task}\left(\mathbf{P}_{vid}\right)\right) \tag{16}$$

For this purpose, we found the Constriction Factor Particle Swarm Optimization (CPSO) [14], [15] to be a good algorithm that robustly finds good optimum positions and performs better than other optimization approaches, like evolutionary algorithms, in terms of computation time.

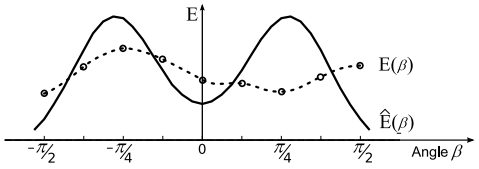

Fig. 7. Observed face illumination distribution $E(\beta)$ and desired distribution $\hat{E}(\beta)$. A good illumination for faces should be symmetrical and stronger from the side than in the front. A quality measure is defined based on the difference of E and $\hat{E}$.

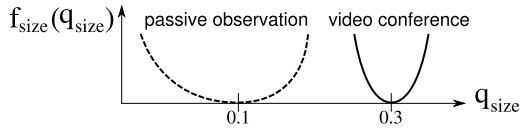

Fig. 8. Two occurrences of the nonlinear transfer function for the relative person size q_{size} with respect to two different observation tasks. An optimal value for a passive observation task is smaller than for a video conference, while a larger tolerance region is admissible for passive observation. This is reflected by the two different cost functions.

V. Experimental Results

We present experimental results that prove the ability of the proposed approach to find a good observation pose and illustrate the need to take into account the scene illumination. A typical situation is regarded here: a person is sitting in front of a table with a window in the background. In order to demonstrate the task dependency of the optimal observation pose, the optimization process was applied for a video conference task and a passive observation task, respectively. The impact of considering illumination is highlighted by doing each optimization once with and once without including the illumination in the quality function (i.e., only the areal conditions, orientation and image composition and "other" factors from subsection IV-A remain).

Fig. 9 shows results for the optimal pose in the context of a video conference task. The optimization was done 80 times, in order to show the stability of the optimization algorithm, the found optimal locations of all runs are marked as dots. Optimization without consideration of the illumination results in an optimal pose directly in front of the person (green dots), the respective camera image is shown in Fig. 9(b). Inclusion of illumination metrics in the optimization prefers a slightly offset position (red dots), which allows a better image quality, as can be seen in Fig. 9(c). In addition to the proposed observation position, the optimal aperture angle is shown for selected poses.

The same examinations were done for the passive observation task. The results are shown in Fig. 10. Note that the optimal pose is not the same as in the video conference task, due to different definitions of the task-dependent transfer functions for quality metrics. Without consideration of lighting, four different possible locations were found (green dots in Fig. 10(a)). All of them are near walls and have similar quality values Q. However, the two left-most positions result in inferior image quality due to strong glare effects (Fig. 10(b)). With the integration of illumination metrics in the optimization criterion, only the two right-most positions are found to be optimal. A resulting camera image is shown in Fig. 10(c).

VI. Conclusions and Future Works

In this paper, we described a novel approach for a task dependent observation pose optimization for indoor living space. Beside the areal conditions and poses of actors, it was demonstrated that an illumination model is necessary for a planning behavior and good image quality results. The update of the illumination model can be done easily by the use of a sequence of exposures with a standard camera, avoiding the need for special light measurement hardware. The optimization process – and therefore the planning time – with a particle swarm optimization is very fast and can be done within fractions of a second. As a next step, we will verify the promising experimental results in a combination with a reactive (model free) image quality assessment on an autonomous robot under real-life conditions.

For the future, there are interesting extensions for the optimization to be examined: With known effect of room

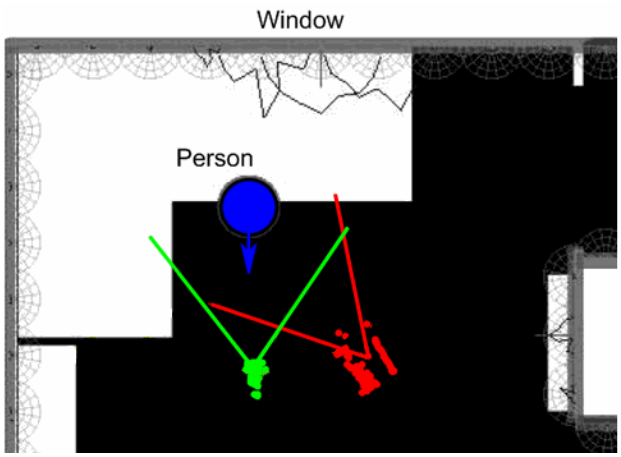

(a) Proposed optimal observation locations are marked with dots (green = without considering illumination, red = including illumination metrics, 80 independent runs each). Orientation and aperture angle are shown for two representative poses. With inclusion of the illumination metrics, a position lateral to the person is preferred to minimize glare from the background light.

(b) Image from a frontal pose (green dots). Backlight glare causes low face contrast and an unbalanced light distribution.

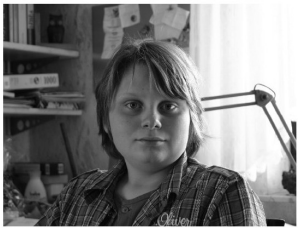

(c) Image from side position (red dots) and with reduced aperture angle, decreasing the number of oversaturated pixels and resulting in improved image quality.

Fig. 9. Pose optimization results for video conference task.

lights and roller blinds on the illumination, in a "smart home" the robot will be able to influence the lighting to obtain best image quality. Furthermore, a better observable pose can be determined, if no observation pose is available for the current user's position, and the robot can give positioning directions to him/her. That way, the robot would undertake even more of the tasks of a real cameraman.

REFERENCES

[1] Bodor, R., Drenner, A., Janssen, M.,Schrater, P. and Papanikolopoulos, N., Mobile Camera Positioning to Optimize the Observability of Human Activity Recognition Tasks, *Int. Conf. Intelligent Robots and Systems (IROS)*, 2005, pp. 1564–1569

[2] Huang, Q., Cui,Y. and Samarasekera, S., Content Based Active Video Data Acquisition Via Automated Cameramen, *Int. Conf. Image Processing*, 1998, pp. 808–812

[3] Ellenrieder, M. M., Optimal Viewpoint Selection for Industrial Machine Vision and Inspection of Flexible Objects, *VDI Verlag GmbH, University of Bielefeld*, ISBN: 3-18-376310-9, 2005

[4] Trucco, E., Model–Based Planning of Optimal Sensor Placements for Inspection, *IEEE Trans. Robotics and Automation*, vol. 13, num. 2, April 1997, pp. 182–194

[5] Schroeter, Ch., Boehme, H.-J. and Gross, H.-M., Memory-Efficient Gridmaps in Rao-Blackwellized Particle Filters for SLAM using Sonar Range Sensors, *Eur. Conf. Mobile Robots*, 2007, pp. 138–143

[6] Schroeter, Ch., Koenig, A., Boehme, H.-J and Gross, H.-M., Multi-Sensor Monte-Carlo-Localization Combining Omnivision and Sonar Range Sensors. *Eur. Conf. Mobile Robots*, 2005, pp. 164-169

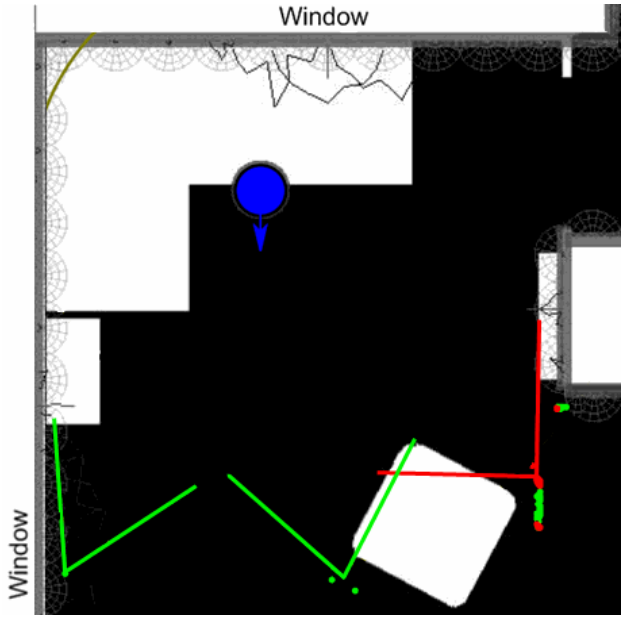

(a) Optimized locations for a passive observation task (green = without considering illumination, red = including illumination metrics, 80 independent runs each). Unlike in the video conference task, a larger variety of good positions exists.

(b) Image captured from the left-most pose in Fig. 10(a) (optimization result without illumination): The person is hardly visible.

(c) Image captured from the right pose in Fig. 10(a): contrast and total image quality are clearly improved.

Fig. 10. Results for passive observation task

[7] Gross, H.-M., Boehme, H.-J., Schroeter, Ch., Mueller, St., Koenig, A., Martin, Ch., Merten, M. and Bley, A. ShopBot: Progress in Developing an Interactive Mobile Shopping Assistant for Everyday Use. *IEEE Int. Conf. Systems, Man and Cybernetics*, 2008, pp. 3471-3478

[8] Mueller, St., Schaffernicht, E., Scheidig, A., Boehme, H.-J. and Gross, H.-M. Are you still following me? *Eur. Conf. Mobile Robots*, 2007, pp. 211-216

[9] Martin, Ch., Gross, H.-M. A Real-time Facial Expression Recognition System based on Active Appearance Models using Gray Images and Edge Images. *IEEE Int. Conf. Face and Gesture Recognition*, 2008, paper no. 299

[10] Marchand, E., Control Camera and Light Source Positions using Image Gradient Information, *IEEE Int. Conf. Robotics and Automation (ICRA)*, 2007, pp. 417-422

[11] DeCusatis, C., Handbook of Applied Photometry, AIP Press, ISBN: 978-1563964169, 1997

[12] Haraldsson, H.B. and Tanaka, M. and Okutomi, M., Reconstruction of a High Dynamic Range and High Resolution Image from a Multi-sampled Image Sequence, *Int. Conf. Image Analysis and Processing*, 2007, pp. 303-310

[13] Won-ho, Cho and Ki-Sang, Hong, Extending dynamic range of two color images under different exposures, *Proceedings of the 17th Int. Conf. Pattern Recognition*, 2004, vol. 4, pp. 853-856

[14] Eberhart, R.C. and Shi, Y., Particle swarm optimization: developments, applications and resources, *Int. Congress on Evolutionary Computation*, 2001, pp. 81-86

[15] Mendes, R. and Kennedy, J. and Neves, J., The fully informed particle swarm: simpler, maybe better, *IEEE Trans. Evolutionary Computation*, June 2004, vol. 8, num. 3, pp. 204-210